

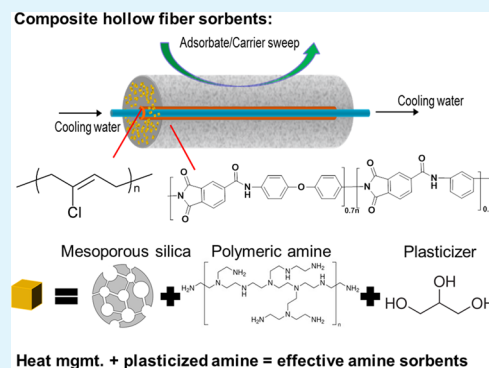
Poly(amide-imide)/Silica Supported PEI Hollow Fiber Sorbents for Postcombustion CO₂ Capture by RTSA

Ying Labreche, Yanfang Fan, Fateme Rezaei, Ryan P. Lively, Christopher W. Jones,* and William J. Koros*

School of Chemical & Biomolecular Engineering, Georgia Institute of Technology, 311 Ferst Drive NW, Atlanta, Georgia 30332-0100, United States

ABSTRACT: Amine-loaded poly(amide-imide) (PAI)/silica hollow fiber sorbents are created and used in a rapid temperature swing adsorption (RTSA) system for CO₂ capture under simulated postcombustion flue gas conditions. Poly(ethylenimine) (PEI) is infused into the PAI/mesoporous silica hollow fiber sorbents during fiber solvent exchange steps after fiber spinning. A lumen-side barrier layer is also successfully formed on the bore side of PAI/silica hollow fiber sorbents by using a mixture of Neoprene with cross-linking agents in a post-treatment process. The amine loaded fibers are tested in shell-and-tube modules by exposure on the shell side at 1 atm and 35 °C to simulated flue gas with an inert tracer (14 mol % CO₂, 72 mol % N₂, and 14 mol % He, at 100% relative humidity (RH)). The fibers show a breakthrough CO₂ capacity of 0.85 mmol/g-fiber and a pseudoequilibrium CO₂ uptake of 1.19 mmol/g-fiber. When tested in the temperature range of 35–75 °C, the PAI/silica/PEI fiber sorbents show a maximum CO₂ capacity at 65 °C, owing to a trade-off between thermodynamic and kinetic factors. To overcome mass transfer limitations in rigidified PEI infused in the silica, an alternate PEI infusion method using a glycerol/PEI/methanol mixture is developed, and the CO₂ sorption performance is improved significantly, effectively doubling the functional sorption capacity. Specifically, the glycerol-plasticized sorbents are found to have a breakthrough and equilibrium CO₂ capacity of 1.3 and 2.0 mmol/g of dry fiber sorbent at 35 °C, respectively. Thus, this work demonstrates two PAI-based sorbents that are optimized for different sorption conditions with the PAI/silica/PEI sorbents operating effectively at 65 °C and the PAI/silica/PEI-glycerol sorbents operating well at 35 °C with significantly improved sorption capacity.

KEYWORDS: hollow fiber sorbent, flue gas, CO₂ capture, PAI, PEI, RTSA



INTRODUCTION

CO₂ capture technology retrofitted to the existing energy infrastructure offers the potential to meaningfully reduce worldwide CO₂ emissions in the near term in a practical manner.^{1–7} The primary technology for CO₂ capture from large point sources, liquid amine absorption, has been widely studied;^{5,8–10} however, the corrosive properties of the amine solutions and intensive energy needs of this process drive the search for alternative approaches.¹¹ The regeneration energy requirement for CO₂ capture using solid sorbents can be significantly reduced relative to classical aqueous amine-based absorption processes due to the absence of large amounts of water and the elimination of water evaporation losses from the aqueous amine stream.^{8,12}

Aminosilicas are a class of organic/inorganic hybrid materials that can be created by several routes, including co-condensation of an aminosilane with silica precursors,¹³ the direct grafting¹⁴ of aminosilanes on a presynthesized silica surface (class 2 materials),¹⁵ via impregnation of presynthesized amine-containing molecules such as amine polymers like poly(ethylenimine) (PEI; class 1 materials)¹⁶ or via direct, in situ polymerization of amine polymers on the support (class 3

materials).^{17–19} Due to their synthetic simplicity, aminosilicas have been extensively studied in separations and catalysis.^{20–30}

For applications in CO₂ adsorption from flue gases, amine sorbents present advantages, such as tolerance to water vapor, but also challenges, such as high heats of adsorption relative to physisorbents such as zeolites or carbons.¹² Like any solid sorbent, the material must also be matched with an appropriate, scalable process configuration if large-scale applications like CO₂ capture from flue gases are to be considered. Fixed beds that are often utilized on the laboratory scale^{31,32} are inappropriate on large scales for this application due to pressure drop and heat transfer issues; for this reason, looping bed designs are often considered.³³ Rapid temperature swing adsorption (RTSA) is an alternate, promising process for CO₂ capture from flue gases. In this approach, polymer/sorbent hollow fibers can be used as microscopic shell and tube heat exchangers to simultaneously allow excellent gas–solid contacting (shell side gas flow) with good heat recovery (via

Received: August 12, 2014

Accepted: October 2, 2014

Published: October 2, 2014

heat transfer to/from bore side fluids) and minimal pressure drop.

Cellulose acetate (CA)/zeolite 13X hollow fiber sorbents were the initial polymer-oxide composite employed in 2009 in an RTSA process for separation of CO₂ from dilute gases.³⁴ This initial “proof of concept” study required dry feed conditions due to the hydrophilicity of the sorbent 13X, which would preferentially adsorb water over CO₂ from a humid gas stream. Subsequently, solid amine sorbents were considered in an RTSA process, which can potentially help overcome disadvantages of aminosilica sorbents, such as their high heat of adsorption. Water-tolerant amine-loaded CA polymer/silica hollow fiber sorbents for postcombustion CO₂ recovery were recently created by utilizing a postspinning amine infusion technique to add amines to silica/polymer hollow fibers by impregnation of PEI³⁵ or grafting of aminosilanes.³⁶ The dynamics of adsorption and desorption over these CA polymer/silica hollow fiber sorbents has also been reported recently.³⁷

In such an RTSA system, mass transfer between the thermal fluids in the bore and the sorbents in the wall of the fiber can be restricted^{34,38} using a lumen barrier layer in the bores. A post-treatment technique for coating the bores based on passage of a polymer latex through the fiber bores has been reported previously.³⁹ For the lumen layer to be defect-free, the cast latex must form a continuous, dense film, and Lively et al. have previously demonstrated a defect-free barrier layer formation on the bore side of cellulose acetate/zeolite 13X hollow fiber sorbents using poly(vinylidene chloride) (PVDC).³⁹ PVDC has unusually low gas and water permeability due to its low fractional free volume and crystallinity; however, it is thermally unstable above about 120 °C due to facile dehydrochlorination. On the other hand, Neoprene latex [poly(chloroprene) (DuPont Elastomer, Wilmington, DE)] can also be formed into a stable, defect-free barrier layer via fiber post-treatment, followed by stabilization by cross-linking^{40,41} of the deposited layer. In this work, three new advances in the development of aminosilica/polymer composite hollow fibers for CO₂ capture in an RTSA configuration are demonstrated: (1) use of a more thermally stable polymer for fiber formation, (2) creation of a more stable bore side lumen layer using Neoprene, and (3) coloaded of hydrophilic, hydroxyl-bearing organic species with the amines to enhance amine efficiency in binding to CO₂ in the composite sorbents.

CA is not a very thermally and oxidatively stable polymer, so an alternative polymer with improved properties, such as the poly(amide-imide) (PAI, Torlon, Solvay Advanced Polymers) could provide important stability advantages. Torlon 4000T is a commercial engineering polymer that was specifically designed to be chemically resistant, thermally stable ($T_g = 278$ °C), and mechanically durable.⁴² The chemical structure of Torlon 4000T is shown in Figure 1. In previous work focused on membranes rather than sorbents, Torlon has been shown to allow high inorganic filler loadings with good particle dispersions in a mixed matrix type structure.^{44–46}

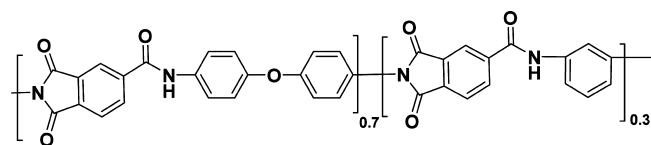


Figure 1. Structure of Torlon 4000T poly(amide-imide).⁴³

Table 1 summarizes the properties of Torlon 4000T PAI compared with Ultem 1010 poly(etherimide) and other

Table 1. Physical Properties of Torlon 4000T PAI, Other Poly(imides), and CA

membrane material	T_g (°C)	contact angle (H ₂ O), (deg)	density (g/cm ³)
Torlon 4000T ⁴⁷	278	87.3	1.38
Ultem1010 ⁴⁸	218	92.6	1.27
Matrimid poly(imide) ^{49,50}	317	91.4	1.23
P84 copoly(imide) ⁵¹	315	82.7	1.36
CA ⁵²	189	64	1.2–1.3

commercially available poly(imides),^{47–51} as well as CA.⁵² CA is the most hydrophilic material among them, with the lowest water contact angle, and our previous work on CA/silica fiber sorbents showed excellent compatibility with silica.³⁵ Torlon, although hydrophobic, has a smaller contact angle than most of the other engineering resins (only slightly higher than that of P84). Adequate hydrophilicity, as indicated by the contact angle data for Torlon, suggests suitable compatibility with silica, and Torlon’s high glass transition temperature will promote stability in RTSA cycles.

Prior researchers have noted the favorable effect of hydroxyl groups in promoting CO₂ adsorption in amine-containing sorbents,^{53–56} and adding poly(ethylene glycol) (PEG) to the PEI/polymer adsorbent is known to accelerate the CO₂ adsorption and desorption rates.^{53,54} Previous work has suggested that enhancement of CO₂ transport rates is associated with the OH groups on the PEG molecules.⁵⁴ It was also suggested that the hygroscopic PEG attracts more water to the adsorbent. Although PEG cannot chemisorb CO₂, it is a well-known CO₂ physisorbent,^{57,58} and the presence of OH groups in PEG may influence the chemical adsorption mechanism using amines. It has been shown that the addition of PEG to amine sorbents can increase the ratio of CO₂ molecules per N atom (referred to as the amine efficiency) to approximately twice the value obtained without the hydroxyl groups, with the formation of carbonate type zwitterions suggested to be promoted.^{53,55} Glycerol has more hydroxyl groups per carbon atom than PEG and has a high boiling point (290 °C), so it was chosen for use as an alternate additive in this work.

Thus, this work reports the development of the first Torlon/aminosilica composite hollow fiber sorbents and explores the formation of cross-linked Neoprene-based lumen layers in the composite material. The enhancement of the amine efficiency by addition of hydroxyl-containing species such as glycerol to the aminosilica particles within the polymeric fibers is also reported for fiber sorbents for the first time.

EXPERIMENTAL SECTION

Materials. PAI (Torlon, Solvay Advanced Polymers, Alpharetta, GA), and poly(vinylpyrrolidone) (PVP) (MW 55 000; Sigma-Aldrich) were the polymers used for the formation of the hollow fiber sorbents. All polymers were dried in vacuum at 110 °C for 1 day to remove moisture before use. *n*-Methyl-2-pyrrolidone (NMP) (Reagent Plus 99%, Sigma-Aldrich) was used as the solvent for the polymer-spinning dope. Methanol (MeOH) (99.8%, ACS Reagent, Sigma-Aldrich) and hexanes (ACS Reagent, >98.5%, Baker) were used for the solvent exchange portion of the fiber formation process, which occurs after spinning. All solvents and nonsolvents were used as-received with no purification or modification. Poly(ethylenimine) (PEI) (MW 800,

Sigma-Aldrich) was used as the amine source in the postspinning amine infusion step, as discussed below. A commercial silica material C803 (W.R. Grace), which was the most suitable silica in our previous CA work,³⁵ was used in this work. Glycerol was used as an additive to PEI/methanol amine infusion solution to enhance the sorbents CO₂ capacity. Neoprene was obtained from DuPont Elastomers, Wilmington, DE, and the cross-linking reagent (TSR-633) was from Tiarco Chemical, Dalton, GA.

Fiber Formation. A typical spinning dope-contained polymer (PAI), sorbent particles, NMP (solvent), water (nonsolvent), and additives (PVP). The polymers and silica were dried at 110 °C in a vacuum oven overnight prior to use. Silica was added to 80% of the required NMP/water components for the dope and sonicated using a 100 W sonication horn. The mixture was stirred and sonicated alternately for 1 h to obtain a well-dispersed suspension. A “prime” dope was made from 20% of the polymers and 20% of the required NMP/water and was stirred for 48 h on a roller prior to sonication of the silica-containing dope. The dispersed silica mixture and prime dope were then mixed together. This mixture was stirred and sonicated alternately for 1 h, and then the rest of the polymer was added and mixed with a mechanical stirrer for 4 h at 50 °C to completely dissolve the polymer and form the final spin-ready dope. The hollow fibers were formed using a nonsolvent phase inversion technique commonly referred to as “dry-jet/wet-quench spinning”.⁵⁹ After several initial tests, the selected final polymer dope solution conditions were chosen and these parameters are listed in Table 2.

Table 2. Comparison of PAI/Silica and CA/Silica Spinning Dope Compositions

	PAI		CA ³⁵
	50 wt %	60 wt %	57 wt %
polymer	14.01	13.09	10.09
PVP	3.92	3.66	4.05
silica (C803)	14.01	19.63	13.38
NMP	59.93	56.01	64.19
water	8.13	7.61	8.29

The CA dope composition is listed for comparison to illustrate the quite different compositions required for the different polymers used here. When the previous CA composition was used the dope was too dilute, and the fiber phase separation step could not be completed effectively. Dope viscosity is critical for spinning as well, so a series of candidate dope concentrations with progressively higher Torlon concentration were considered to arrive at a dope that could be extruded to form a continuous strand when immersed in a quench bath. This optimization could be done efficiently with relatively small amounts of dope in a simple 30 cm syringe with a nozzle.

The selected spinning dope was coextruded with a bore fluid through a spinneret into a nonsolvent water quench bath to induce phase separation and form a porous fiber. A bore fluid comprising 80% NMP and 20% H₂O was used on the basis of prior experience that it provided a more-or-less “neutral” fluid to form a stable bore in the nascent fiber. Fibers were collected on a take-up drum and finally removed from the drum using a sharp blade. These fibers were placed in a bath of deionized water for 1 week, and the water was changed every day, to remove traces of residual solvent. After the last day, the fibers (approximately 75 g) were solvent exchanged by immersing them in three successive aliquots (400 mL) of methanol for 20 min each to avoid pore collapse, which would occur if they were dried directly with water-filled pores. The fibers were removed from the bath and allowed to dry in a fume hood in air for 1 h, then they were placed in a vacuum oven and dried for 2 h at 100 °C. The complete spinning conditions are given in Table 3. PAI/silica fibers used a spinneret temperature of 50 °C, rather than the 25 °C spinneret temperature that had been found to provide reliable spinning for CA/silica fibers.³⁵

Postspinning Infusion of PEI in Fiber Sorbents. The postspinning infusion of PEI into CA/silica fibers was described in

Table 3. Torlon/Silica Composite Fiber Spinning Parameters

air gap height	3 cm
take-up rate	5–20 m/min
quench bath medium and temperature	H ₂ O, 50 °C
spinneret temperature	50 °C
bore fluid composition	80/20 (wt %), NMP/H ₂ O
extrusion rate	core, 800 mL/h; bore, 300 mL/h

detail in our previous work.³⁵ After spinning the fibers, the fibers were subjected to a methanol solvent exchange process, as noted above, followed by treatment in PEI/methanol or PEI/glycerol/methanol, and then the fibers were dried at room temperature for 1 h in a fume hood and at 70 °C for 2 h in a vacuum oven. The amine recharging procedure for deactivated fibers was the same as described in our previous work.³⁵

Materials Characterization. A thermogravimetric analyzer (TA Instruments SDT Q500) was used for ex-situ CO₂ adsorption characterization using a 10% CO₂/90% N₂ gas mixture at 1 atm. The samples were heated first to 120 °C under He flow to remove moisture and CO₂ adsorbed from the air and then cooled to 35 °C under He flow. CO₂ containing gas (90 mL/min) was flowed over the samples during the sorption tests. A weight gain was observed due to CO₂ sorption in the sample, and the uptake per gram dry silica or dry fiber (mmol/g-fiber) was calculated as the CO₂ capacity.

Scanning electron microscopy (SEM, Leo 1530, Leo Electron Microscopy, Cambridge, UK) was used to evaluate the fiber sorbent morphology. The samples were sputter-coated with a 10–20 nm thick gold coating (Model P-S1, ISI, Mountain View, CA) before being transferred to the SEM for imaging. Elemental analysis was performed by Columbia Analytical Services, Inc. (Kelso, WA).

Fiber Module Characterization in a Simulated Flue Gas Flow System. Fibers containing 50 wt % silica impregnated with PEI were cut and mounted in 11 in. long modules composed of 3 fibers per module. Characterization of the fiber modules was performed in a simulated flue gas flow system, as reported in our previous work.³⁷ Three T-type hypodermic thermocouples (TC) (located at $z/z_0 = 0.3, 0.5,$ and 0.7) were placed in the module to measure the temperature profiles of fiber sorbent at various locations during the experiment. The fiber module was degassed under flowing N₂ at 90 °C using external heating tape prior to CO₂ adsorption tests. Adsorption experiments were carried out by flowing a simulated flue gas (14 mol % CO₂, 68 mol % N₂, 14 mol % He, at 100% RH) through the shell side of the temperature-controlled hollow fiber adsorbent module at 40 mL/min at 35 °C, 1 atm (gas space hourly velocity, 1000 h⁻¹). Helium was used as an inert tracer, N₂ acted as the carrier gas, and CO₂ was the adsorbate of interest. The concentration of CO₂ at the module outlet was transiently measured by mass spectrometry (ultrahigh vacuum Pfeiffer Vacuum QMS 200 Prisma Quadrupole Mass Spectrometer) until equilibrium was reached. The total CO₂ uptake was determined by integrating the area bounded by the CO₂ and He elution molar flow rate fronts (the He tracer accounts for the mean residence time within the system).

Lumen Layer Latex Formation. A modification of our prior Neoprene lumen layer formation technique⁴⁰ was required in this study that used fibers with particles in the sorbent wall. In the earlier work with ionic liquids, a mixture of Neoprene/TSR-633/H₂O latex was used to form a barrier layer in the lumen side of hollow fibers via a post-treatment method.^{39,40} In that case, a mixture of Neoprene/TSR-633/H₂O (water 15 wt %) yielded good results for neat Torlon fibers;⁴⁰ however, this 15 wt % solution failed for these materials and led to consistent fiber bore plugging in the particle-laden fibers. The ratios of Neoprene/TSR-633/H₂O were optimized systematically using three-fiber sorbents potted into an 11 in. stainless steel module. The module was connected to a post-treatment system in a vertical position (Figure 2), and latex was extruded through the fibers during the lumen layer formation, as shown in Figure 3. Water-saturated nitrogen at 20 psig was then connected to the module for 1 h. The

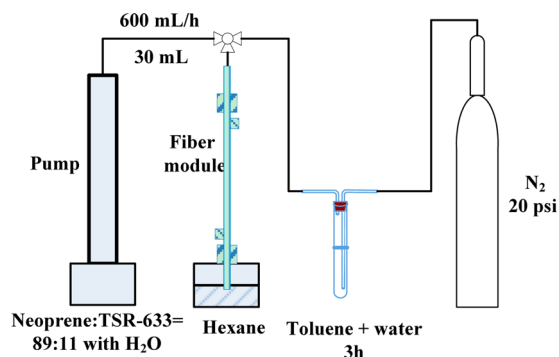


Figure 2. Schematic of the lumen layer post-treatment system.

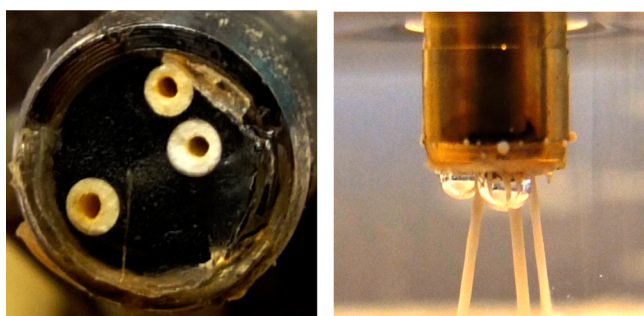


Figure 3. Photographs of (left) the cross-section of the hollow fiber sorbent module end and (right) latex jets extruding from the hollow fibers into the hexane bath.

optimum mixture of Neoprene/TSR-633 (89/11 by weight) and water with a weight ratio from 85/15 to 70/30 were extruded into the bores of the fiber at a flow rate of 600 mL/h, with 30 mL latex per fiber using an Isco syringe pump (Model 1000D, Teledyne Isco). The fiber end was immersed in a hexane bath during the post-treatment process to inhibit the rapid drying and possible plugging of the fiber exit by latex.^{39,40} The barrier layer was then dried in the previously described “toluene-assisted” mode by flowing 20 psig toluene-water saturated nitrogen in the bores of the fiber module for 3 h. The “toluene-assisted” mode allows the lumen layer to form a dense, continuous layer in the bores of the fiber,^{39,40} and the opposite end of the fiber module was post-treated using the same procedure.

RESULTS AND DISCUSSION

Torlon/Silica Hollow Fiber Characterization. Electron micrographs of PAI/silica fiber sorbents are shown in Figure 4. From the SEM images, the fibers qualitatively possess the

desired highly porous state. Furthermore, the bores are centered, as shown in Figure 4 (left). The right side of Figure 4 shows a magnified image of the fiber, which depicts the dispersed nature of the silica particles and the porosity of the PAI fiber. The fiber wall thickness was approximately 300–400 μm , as shown in Figure 4, which has previously been shown to provide sufficient sorption capacity while still ensuring rapid mass transfer in fiber sorbents.³⁵

The CO_2 capacities of PAI/silica and post infused PAI/silica/PEI hollow fiber sorbents, as measured via thermogravimetric analysis (TGA), are shown in Table 4. Two silica loadings (50

Table 4. CO_2 Capacities of 50 and 60 wt % Silica/PAI/PEI Fibers

fiber	CO_2 capacity (mmol/g-fiber) ^a
60 wt % silica/PAI fiber	$0.12 \pm 0.07^{b,c}$
50 wt % silica/PAI/PEI	1.10 ± 0.05^b
60 wt % silica/PAI/PEI	1.25

^aFrom CO_2 adsorption using dry, 10% CO_2 via TGA. ^bError bars represent testing of two different batches of fibers. ^cTorlon/silica fibers without PEI have a CO_2 capacity of 0.12 mmol/g-fiber due to CO_2 physisorption.

and 60 wt %) used in the PAI/silica/PEI fiber sorbents were found to have CO_2 capacities of 1.10 and 1.25 mmol/g-fiber, respectively. The 50 wt % silica/PAI//PEI fiber sorbent results are similar to the 57 wt % CA/silica/PEI fiber sorbents reported previously;³⁵ however, the higher silica loading Torlon fibers have a higher CO_2 capacity, as more PEI could be infused into the higher silica-loaded fibers. Unfortunately, the 60 wt % silica/PAI//PEI fiber sorbents were more brittle and difficult to process into modules, so the 50 wt % silica/PAI//PEI fiber sorbents were used to coat lumen layers for further testing.

We have previously investigated the textural properties of the fiber-supported silicas before and after postspinning infusion and have found that, in the case of PEI impregnation, the pore volume of the silica was mostly occupied by PEI,³⁷ while the polymer pores were largely unaffected by the presence of PEI. This is to be expected on the basis of the relatively small size of the silica pores compared to the polymer porosity. We have also previously used elemental analysis to measure the weight loading of amines in the fiber-supported silicas, and have confirmed that good amine loadings in the silica were achieved via the postspinning infusion technique.³⁵ Elemental analysis demonstrated that 50 wt % silica PAI/silica has nitrogen and

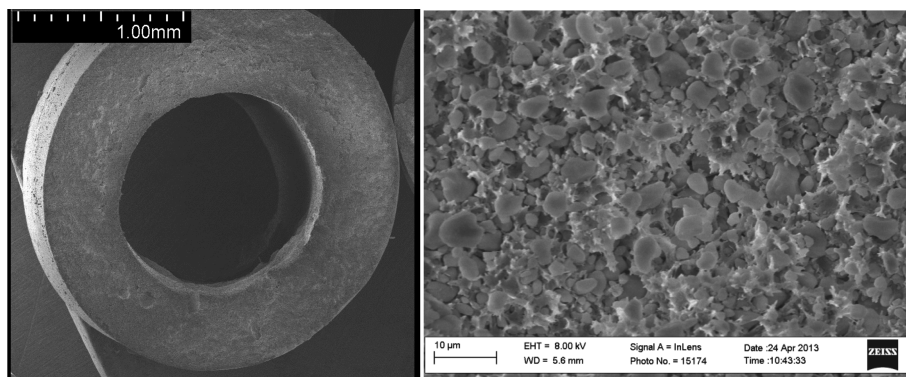


Figure 4. SEM images of PAI/silica hollow fiber sorbent: (left) cross section and (right) magnified image of fiber porosity with embedded silica particles.

silicon loadings of 3.49 and 6.41 mmol/g-fiber, respectively. After the PEI infusion, the PAI/silica fiber elemental nitrogen concentration increased to 8.48 mmol/g-fiber (silicon loading 4.73 mmol/g-fiber) from 3.49 mmol/g-fiber, reflecting an increase of 5.90 mmol/g-fiber.

The CO₂ capacities of 50 wt % silica/PAI/PEI hollow fibers prepared under different amine infusion conditions were evaluated, and the results are reported in Table 5 for the

Table 5. CO₂ Capacities of 50 wt % Silica/PAI/PEI Hollow Fibers Prepared under Different Amine Infusion Conditions (TGA Using 10% CO₂)

infusion time	CO ₂ capacity, mmol/g-fiber			
	PEI concentration in methanol			
	5%	8%	10%	12%
2 h	0.67	0.94	1.11	1.09
4 h	0.63	1.06	1.05	0.97
20 h	0.63	0.96	1.09	0.84

array of 2–20 h infusion times. The fiber infused in 10% PEI/methanol for 2 h gave the highest CO₂ capacity (1.10 mmol/g-fiber), and longer infusion times did not produce further capacity increase. This observation is consistent with our previous experiments that investigated the effect of infusion time in detail.³⁵ The uncertainty of these tests is about ± 0.04 mmol/g-fiber based on multiple infusion runs under identical conditions. These results are similar to the CA/silica/PEI fiber sorbents reported previously,³⁵ as expected. However, these fibers should be more useful in aggressive flue gas conditions with humid SO_x and NO_x present, due to the more robust nature of Torlon relative to CA. Moreover, if capacity loss occurs after many cycles, recharging of PEI can be achieved,³⁵ and the CO₂ capacity of the recharged sample (1.10 mmol/g-fiber) was equal to the original fiber.

PAI/Silica/PEI Hollow Fiber Module Breakthrough and Equilibrium CO₂ Capacities. Three amine-loaded fibers prepared via the optimal conditions described in the Experimental Section were assembled into shell-and-tube modules and exposed on the shell side to simulated flue gas with an inert tracer (14 mol % CO₂, 14 mol % He, 72 mol % N₂, at 100% relative humidity (RH)) at 1 atm and 35 °C. The sorption results in Figure 5 depict the CO₂ breakthrough curve, with the helium tracer (Figure 5, left) and corresponding temperature release profiles (Figure 5, right). As the CO₂ front propagated through the module, the inert helium tracer filled the void spaces of the fiber sorbent and was subsequently

displaced by CO₂ and pushed out of the module in a typical “roll-up” effect,⁶⁰ which is indicative of rapid mass transfer in the fiber sorbent. Under humid conditions, the fibers were found to have a breakthrough⁶¹ CO₂ capacity (q_b) of 0.85 mmol/g-fiber, with a mass transfer propagation front velocity of 0.21 cm/s. The humid CO₂ pseudoequilibrium uptake⁶¹ (q_{pe}) at 1 atm and 35 °C was 1.19 mmol/g-fiber. These results are considerably higher than for the CA/silica/PEI fiber reported in previous work, which had a q_b of 0.67 mmol/g-fiber and q_{pe} of 1.03 mmol/g-fiber.³⁷ It should be noted that the PEI loading of CA/silica/PEI fibers³⁵ and PAI/silica/PEI fibers are 5.2 mmol/g-fiber³⁵ and 5.9 mmol/g-fiber, respectively. Thus, the higher sorption capacities are associated with higher amine loading in the PAI/silica/PEI case, as the amine efficiencies for q_{pe} for both the CA/silica/PEI fibers and PAI/silica/PEI fibers were 0.20 (CO₂/PEI molar ratio). In the PAI/silica/PEI fibers, there are 4.73 mmol silica/g-fiber and 5.90 mmol PEI/g-fiber (Table 5). These figures mean that there are 0.331 g silica and 0.253 g PEI per 1 g-fiber. Because the PEI density is ~ 1.08 g/mL, there is 0.234 cm³ PEI/g-fiber. Because the silica pore volume is 0.85 cm³/g-silica,³⁵ the PAI/silica fiber had a silica pore space of 0.281 cm³/g. Therefore, 83.3% of the silica pore space of the fiber was filled with PEI, estimated as the ratio of PEI 0.234 cm³/g-fiber divided by silica pore volume 0.281 cm³/g-fiber.

For breakthrough capacities, the amine efficiency (0.14) for q_b for the PAI/silica/PEI fibers was also similar to that of the CA/silica/PEI fibers (0.13). Thus, it seems the microstructures of these two kinds of fibers may be only subtly different, thereby affecting the incorporated amine amounts and breakthrough properties under these experimental conditions. It should be noted that the influence of silica materials with different porosities on CO₂ sorption was studied previously.³⁵

The sorption enthalpy release was estimated by the thermal response, and the thermal front propagation velocity was 0.22 cm/s. The local temperature increased about 2–4 °C due to the exothermic CO₂ adsorption as shown in Figure 5, right. Finally, the water breakthrough capacity was found to be 6.0 mmol/g-fiber, while the pseudo equilibrium water uptake was 10 mmol/g-fiber.

The adsorption of CO₂ by the PAI/silica/PEI adsorbents is driven mainly by exothermic chemical reaction between the acidic CO₂ molecules and the basic amine groups within the PEI molecules. Thus, the equilibrium CO₂ adsorption capacity should be lower at higher operating temperatures due to the exothermic nature of this process.⁶² With this in mind, the PAI/silica/PEI fiber sorbents modules were evaluated with regard to the effect of operating temperature on the performance of the adsorbent. Isothermal TGA-determined CO₂ sorption capaci-

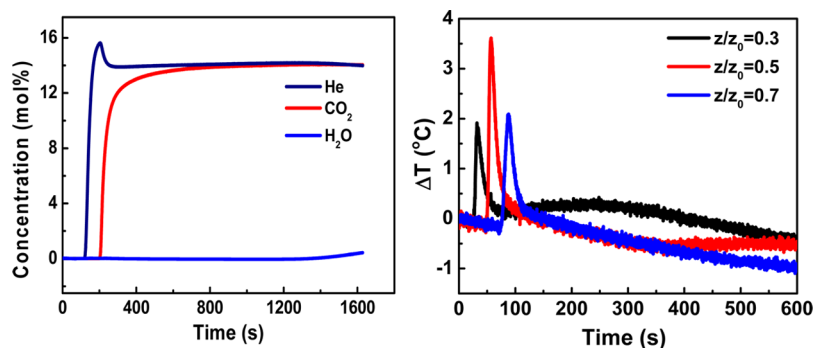


Figure 5. PAI/silica/PEI hollow fiber (left) breakthrough curve and (right) temperature release profiles.

ties of CA/silica/PEI³⁷ and PAI/silica/PEI at various operating temperatures between 35 and 75 °C were measured, and the results are shown in Figure 6. The CA/silica/PEI and PAI/silica/PEI fiber sorbents showed a maximum capacity at 45 and 65 °C, respectively.

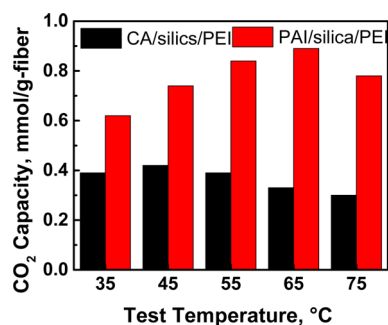


Figure 6. Effects of sorption temperature on the CO₂ breakthrough capacity of CA/silica/PEI PAI/silica/PEI sorbents at 10% CO₂ concentration under dry conditions.

From 35 to 65 °C, the increasing trend of CO₂ adsorption capacity with an increase in operating temperature is counter-intuitive for exothermic adsorption. However, for PEI-impregnated silica sorbents, this trend is well-established and is associated with a trade-off between diffusion effects (better at elevated temperatures) and adsorption effects (better at lower temperatures), as noted by Song and co-workers.^{16,53} The CA/silica/PEI fiber shows a weak maximum capacity at 45 °C, reflecting the competing effects of thermodynamic and diffusive factors. On the other hand, as noted above, the more pronounced positive trend in capacity vs temperature suggests the dominance of kinetic diffusion resistance factors for the Torlon-based fiber.

The chemical reaction of CO₂ with PEI typically produces alkylammonium carbamates through a two-step reaction. The acid–base reaction of one molecule of CO₂ and one molecule of amine forms a zwitterionic intermediate that is then deprotonated by another amine molecule to form the final carbamate product. Amundsen et al.,⁶³ for instance, reported that the densities and dynamic viscosities of monoethanolamine solutions increased significantly with increasing CO₂ loading at various temperatures ranging from 25 to 80 °C. The formation of carbamates with PEI significantly increases the density and viscosity of the PEI layer, likely due to polymer chain cross-linking, and inhibits further CO₂ diffusion. At higher temperature, PEI has a lower viscosity and higher molecular mobility, so for CO₂ adsorption at 75 °C, the higher PEI mobility and CO₂ diffusivity reduces resistance for CO₂ access to PEI near the center of the silica particles. Without cooling water in the bore, heat release at the 65 °C sorption temperature is estimated to produce an in situ temperature of around 70–75 °C. At the lower temperature of 35 °C considered earlier, the lower mobility of PEI and the lower CO₂ diffusivity, coupled with the stronger binding constant of amines with CO₂ in more strongly gelled polymers, decreases CO₂ access to PEI deep in the silica pores during realistic breakthrough cycle times. On the other hand, by being able to operate at higher sorption cycle temperatures, the Torlon-based silica fibers make more efficient use of the PEI sorbent throughout the silica particles. The PAI/silica/PEI hollow fiber sorbents, therefore, maintained better access for CO₂ to the amines at higher temperatures,

even at high weight percentage PEI loadings. Thus, these PAI/silica/PEI sorbents demonstrated higher capacities at the relatively high adsorption temperature of 65 °C, which is beneficial to the RTSA process. With these sorbents, the process cycle can swing between 65 and 120 °C, thereby reducing energy costs compared to processes with adsorption at lower temperatures.

Promoting the CO₂ Adsorption of PEI-Infused Fiber Sorbents by Adding Glycerol. We have previously utilized a combined theoretical–experimental approach to understanding the kinetics of adsorption in fiber sorbent materials.³⁷ We identified that adsorption into the bulk PEI phase was strongly dependent on CO₂ loading; however, this loading-dependent diffusion was affected by the system temperature. In the same work,³⁷ we identified that the presence of water in the silica-supported amine sorbents greatly boosted the kinetic uptake of CO₂ by the sorbents. We hypothesized that water acted as a plasticizer for the PEI chains that became rigid after adsorbing CO₂. These observations from previous studies led us to pursue a plasticizer that might not be desorbed under thermal cycling—glycerol.

The above insights regarding the ability of higher temperatures to mitigate diffusion resistances within the PEI held in the sorbent particle revealed an additional opportunity for sorbent improvements. Specifically, by adding a “plasticizer” to increase the CO₂ diffusion coefficient though the gelled PEI at the outer regions of the silica particles, access to the deeply held PEI might be possible, even at low sorption temperatures where equilibrium uptakes tend to be higher. Thus, to enhance the CO₂ capacity and the adsorption/desorption rate, glycerol was added to PEI/methanol infusion solution. The CO₂ capacities of the fiber samples were subsequently assessed via TGA at 10% CO₂ concentrations. Figure 7 illustrates the influence of the glycerol concentration in the 10% PEI/methanol infusion solution on the CO₂ uptakes.

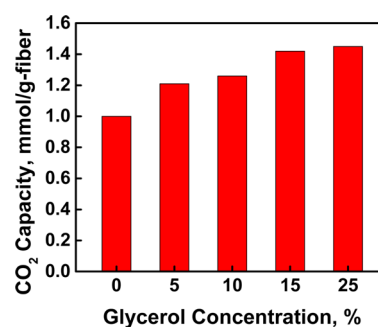


Figure 7. Influence of glycerol concentration in 10% PEI/methanol on CO₂ capacity of resulting sorbents measured at 35 °C using 10% CO₂ via TGA.

The CO₂ capacity increased with the addition of glycerol to the 10% PEI/methanol amine-infusion solution. This result is similar to those of previous researchers who used other hydroxyl-containing additives,^{53–56} whereby the enhancement of the CO₂ capacity is believed to be related to the presence of –OH groups from the glycerol added along with the PEI. The presence of hydroxyl groups in glycerol will also promote water uptake, which has been empirically shown to further increase amine efficiency¹² and may promote the formation of carbonate type zwitterions. On this basis, we expected that the amine groups would sorb more CO₂ and the glycerol-plasticized PEI

would be expected to make the CO₂ more accessible to PEI during breakthrough studies.

To obtain preliminary insight into the cyclic stability of the amine-loaded hollow fiber sorbents with and without glycerol, cyclic TGA experiments were performed under dry conditions by cycling the furnace temperature between 35 and 120 °C and switching the gas between 10% CO₂/N₂ and pure He in adsorption/desorption cycles. Figure 8 shows the cyclic mass

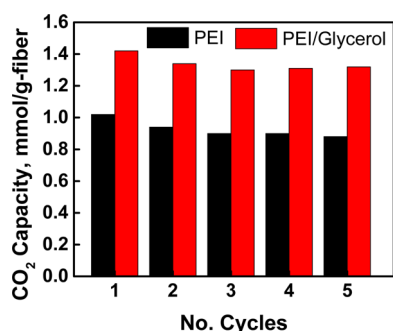


Figure 8. Thermal cycling of PAI/silica/PEI and PAI/silica/PEI-glycerol fiber adsorbents (mmol/g-fiber) at 10% CO₂ concentration at 35 °C.

gain/loss versus time for five cycles, where a cycle is 500 min long. From the figure, it can be observed that the capacity of the PEI infused adsorbents degraded slightly during this cycling. For example, the sorption capacities of the PAI/silica/PEI hollow fibers decreased by 14% over five cycles, from 1.02 to 0.83 mmol/g fiber. This result shows that the PEI-impregnated adsorbent, although having a high initial adsorption capacity, may experience slow capacity loss under dry conditions. This is consistent with studies that used PEI-impregnated amine powders, where urea species formed under dry conditions.^{37,64,65} A slight decrease of CO₂ capacity during each cycle, as shown in Figure 8, might also be attributed to the small losses of water and low molecular weight oligomers from PEI during the heating/desorption steps; however, the overall trend shows good stability. In comparison, the PAI/silica/PEI-glycerol fiber had much higher CO₂ capacity and lower capacity loss over moderate cycling.

Ten glycerol/PEI/methanol (15/10/75 wt %)-infused PAI/silica sorbent fibers were then assembled into a 22 in. long, 1/2 in. outer diameter shell and tube module and exposed on the shell side at 1 atm and 35 °C to simulated flue gas with an inert tracer (14 mol % CO₂, 72 mol % N₂, 14 mol % He (at 100% RH)). The hollow fiber breakthrough behavior is shown in Figure 9. The hollow fiber breakthrough capacity and the equilibrium CO₂ capacity increased by a factor of 1.5 compared to that fiber module infused with PEI without addition of glycerol. The fiber module was also operated in a “prehydrated” mode, whereby a prehumidification step was used to ensure the module was fully saturated with water prior to CO₂ sorption.³⁷ It was then assumed that the amount of water adsorbed on the module remained constant by flowing wet flue gas with 100% RH throughout the CO₂ adsorption test. The data from these sorption runs are listed in Table 6. The uncertainty of this test was about ±0.03 mmol/g-fiber, based on amine multiple infusion studies. The results show that the breakthrough capacity of the fiber containing amines and glycerol increased by 60% compared to the glycerol-free fiber. Interestingly, when the fibers containing glycerol were prehydrated, the results were

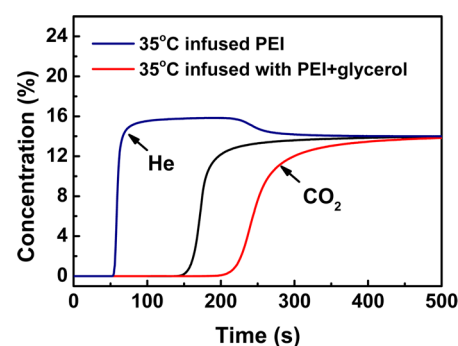


Figure 9. Comparison of breakthrough curves in dual layer PAI/silica/PEI hollow fiber with glycerol vs without glycerol at 35 °C using 14% CO₂.

Table 6. PAI/Silica/PEI Hollow Fiber Breakthrough and Equilibrium CO₂ Capacity at 35 °C Using 14% CO₂

module test condition	CO ₂ , q _b (mmol/g-fiber)	CO ₂ , q _{pe} (mmol/g-fiber)
PAI/Silica/PEI	0.8	1.2
PAI/silica/PEI-glycerol	1.3	2.0
prehydrated PAI/silica/PEI-glycerol	1.3	2.0

the same as for the nonprehydrated fibers, within experimental error. Previous work noted that the breakthrough capacity in prehydrated CA-based fibers increased by 60% compared to a nonprehydrated module.³⁷ As noted above, the observation that moisture improved the sorption capacity of the supported PEI sorbents has been reported in the literature.^{66,67} Thus, in this work, adding glycerol to the PAI/silica/PEI fiber sorbents has the same effect as adding moisture, because both agents plasticize the PEI, and the already plasticized glycerol containing fibers appear to not need added water in the PEI (as provided by the prehydration). Clearly, another benefit of adding the low volatility glycerol (bp 290 °C) is its good long-term stability (Figure 8).

PAI/Silica/PEI hollow fibers with glycerol were also tested at 35 and 65 °C. The breakthrough and pseudoequilibrium CO₂ capacities are listed in Table 7. Both the breakthrough and

Table 7. “Glycerol-Promoted” PAI/Silica/PEI Hollow Fiber Breakthrough and Equilibrium CO₂ Capacity at Different Temperatures

module test condition	CO ₂ , q _b (mmol/g-fiber)	CO ₂ , q _{pe} (mmol/g-fiber)
PAI/silica/PEI-glycerol, 35 °C	1.3 ± 0.02	2.0 ± 0.03
PAI/silica/PEI-glycerol, 65 °C	1.1 ± 0.02	1.7 ± 0.03

pseudoequilibrium CO₂ capacities at 65 °C were lower than those obtained at 35 °C. This observation is also consistent with the hypothesis that glycerol, like water, promotes PEI plasticization, which removed diffusion limitations in the PEI, making the processes thermodynamically controlled, so the temperature increase will reduce the CO₂ capacity in the exothermic process.

Lumen Layer Formation. The preceding section focused on the intrinsic properties of the uncooled fiber sorbents; however, for ultimate utility, as noted earlier, a functional lumen layer is required to enable cooling and heating water flows through the bores in heat integrated cycles. Also as noted earlier, a convenient way to create the lumen side barrier layer

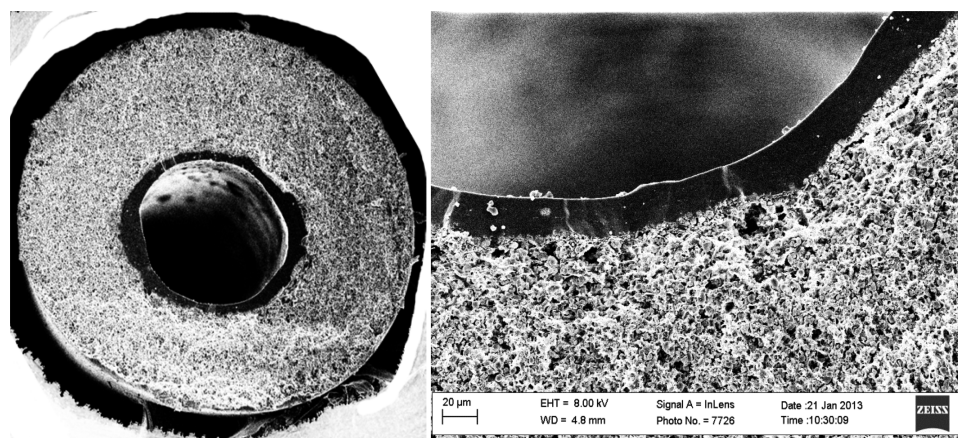


Figure 10. SEM images of Neoprene-coated fiber sorbents focusing on the lumen side barrier layer. (Left) Cross section of fiber sorbent with Neoprene lumen layer and (right) high magnification of the Neoprene layer.

is via a post-treatment technique based on flow of a polymer latex through the fiber bores. In previous work on a Torlon fiber without silica,⁴⁰ a latex composition of Neoprene/TSR-633/H₂O with a weight ratio of 75.6/9.4/15 was used to create a lumen layer. In the present work using PAI/silica fiber sorbents with 50% silica content, the inner layer skin of the fiber bore was much rougher than that of a neat Torlon fiber.⁴⁰ When the Neoprene/TSR-633/H₂O concentration was 75.6/9.4/15, cross-linked agglomerates often formed and plugged the hollow fiber during the coating procedure. The optimized latex composition to limit this formation was a Neoprene/TSR-633/H₂O combination with a weight ratio of 71.2/8.8/20, as noted in the Experimental Section. For water concentrations >20%, the resulting lumen layer was too permeable and allowed excessive water permeation. Once the process was optimized, three fiber sorbents were potted into an 11 in. stainless steel module, and the latex mentioned above was extruded into the fiber at 600 mL/h and 30 mL/fiber. The fibers were dried in “toluene-assisted” mode^{39,40} to give fibers with functional lumen layers.

As observed in the SEM images shown in Figure 10, a ~20 μm thick lumen layer formed successfully in these fibers. Measurements of He and N₂ single gas permeation through the hollow fiber sorbents with and without lumen layers at 35 °C were performed, and the results are listed in Table 8. As

Table 8. He Permeation of the Fiber Sorbents with and without Lumen Layers, 25 psig

sample	He permeance (GPU) ^a	He/N ₂
PAI/silica/PEI	72,000	1.7
PAI/silica/PEI/Neoprene	4.5	4.0

^aGPU = 10⁻⁶ cm³ (S.T.P.)/(s·cm²·cm Hg)

desired, the lumen layer substantially decreased the He permeance of the PAI/silica/PEI hollow fiber sorbent, with an increase in the He/N₂ selectivity beyond the Knudsen diffusion limit of 2.65. Exceeding the Knudsen limit⁶⁸ means that a functional polymer layer lumen has been deposited.

A stainless steel module with three-fiber PAI/silica/PEI sorbents containing lumen layers was then evaluated in the RTSA system with active cooling water in the bore side during CO₂ sorption tests at 35 °C using simulated flue gas (100% RH). The breakthrough curves are presented in Figure 11,

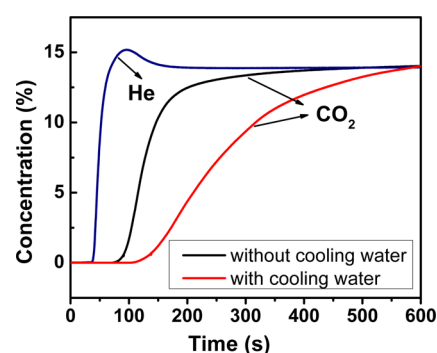


Figure 11. Breakthrough curves without cooling water vs with cooling water in the bore side of a PAI/silica/PEI fiber module at 35 °C using 14% CO₂.

where they are compared against the performance of the same PAI/silica/PEI fibers without cooling water. The CO₂ breakthrough time increased from 75 to 110 s upon addition of cooling water to the bore side, which increased the q_b from 0.43 mmol/g-fiber to 1.04 mmol/g-fiber, as shown in Table 9. It

Table 9. CO₂ Capacity of the PAI/Silica/PEI Hollow Fiber Sorbents with and without Cooling Water at 14% CO₂ Concentration

module type	CO ₂ q_b (mmol/g-fiber)	CO ₂ q_{pe} (mmol/g-fiber)
without cooling water	0.43	1.14
with cooling water	1.04	2.32

should also be noted that the breakthrough profile of the uncooled fiber was sharper. This is most likely due to the “thermal self-sharpening effect”, whereby the local release of heat significantly reduced mass transfer resistances (thus making the front sharper), but at the expense of CO₂ uptake. The CO₂ capacities of the hollow fiber sorbents with a lumen layer were thus shown to be approximately double that of the fibers without lumen layers. As was discussed above, a lower temperature led to lower CO₂ capacity in highly filled PEI-based sorbents in the absence of glycerol plasticization. It is also noted that there is a nonzero permeability of the lumen layer to water vapor,⁴⁰ which could introduce extra moisture in the sorbents during sorption with water flowing in the fiber bores, possibly increasing the sorption capacity of the supported PEI

sorbents.^{37,63} This result is consistent with our previous CA/silica fiber studies with flowing, bore side cooling water, as well as sorption using CA/silica fibers that were prehydrated with water on the shell side.³⁷ In that work, it was discussed that the breakthrough capacity in the prehydrated module increased by 60% compared to the dry module, again showing the positive effect of water on CO₂ sorption on amine sorbents.

CONCLUSIONS

In this work, the previously demonstrated concept of postspinning infusion of PEI into CA/silica hollow fiber sorbents was successfully transferred to a thermally stable, mechanically durable, and chemically resistant PAI/silica/PEI hollow fiber sorbent platform. The desired highly porous fibers were found to have a breakthrough CO₂ capacity of 0.85 mmol/g-fiber and a pseudoequilibrium CO₂ uptake of 1.19 mmol/g-fiber when the modules were exposed on the shell side to simulated flue gas with an inert tracer (14 mol % CO₂, 72 mol % N₂, and 14 mol % He at 100% RH, 1 atm, and 35 °C). These values are higher than the CA/silica/PEI hollow fiber sorbents studied previously due to higher amine loadings achieved in the PAI/silica/PEI hollow fibers. Conditions for coating the fiber bores using Neoprene to create a functional barrier lumen layer were developed and optimized for these PAI/silica/PEI hollow fibers. At 65 °C, the new PAI/silica/PEI fiber sorbents showed their maximum sorption capacity, which is advantageous as it allows the RTSA process design to increase the sorption temperature to 65 °C, which is closer to the feed flue gas and desorption temperatures, allowing for potentially reduced energy cost in RTSA cycling. The new PAI/silica/PEI-glycerol sorbents were found to have a much higher breakthrough and equilibrium CO₂ capacity of 1.3 and 2.0 mmol/g-dry fiber sorbent, respectively, at 35 °C than the glycerol-free sorbents, allowing for substantially enhanced CO₂ capacity and operation at lower temperatures, if desired. The addition of glycerol appears to have a plasticizing effect on the PEI chains, similar to the effect of added water. Overall, the work pushes forward the polymeric hollow fiber-aminosilica platform toward 1 day, allowing for practical operation in RTSA separation processes.

AUTHOR INFORMATION

Corresponding Authors

*E-mail: cjones@chbe.gatech.edu.

*E-mail: william.koros@chbe.gatech.edu.

Notes

The authors declare no competing financial interest.

ACKNOWLEDGMENTS

The authors acknowledge the U.S. Department of Energy, National Energy Technology Laboratory (DOE-NETL) under contract DE-FE0007804 and General Electric (GE) for financial support. However, any opinions, findings, conclusions, or recommendations expressed herein are those of the author(s) and do not necessarily reflect the views of the DOE or GE.

REFERENCES

(1) Littel, R. J.; Versteeg, G. F.; van Swaaij, W. P. M. Physical Absorption into Non-Aqueous Solutions in a Stirred Cell Reactor. *Chem. Eng. Sci.* **1991**, *46*, 3308–3313.

(2) Chiesa, P.; Consonni, S. P. Shift Reactors and Physical Absorption for Low-CO₂ Emission IGCCs. *J. Eng. Gas Turbines Power* **1999**, *121*, 295–305.

(3) Bishnoi, S.; Rochelle, G. T. Absorption of Carbon Dioxide into Aqueous Piperazine: Reaction Kinetics, Mass Transfer and Solubility. *Chem. Eng. Sci.* **2000**, *55*, 5531–5543.

(4) Aroonwilas, A.; Veawab, A. Characterization and Comparison of the CO₂ Absorption Performance into Single and Blended Alkanolamines in a Packed Column. *Ind. Eng. Chem. Res.* **2004**, *43*, 2228–2237.

(5) Rochelle, G. T. Amine Scrubbing for CO₂ Capture. *Science* **2009**, *325*, 1652–1654.

(6) Chang, F. Y.; Chao, K. J.; Cheng, H. H.; Tan, C. S. Adsorption of CO₂ onto Amine-grafted Mesoporous Silicas. *Sep. Purif. Technol.* **2009**, *70*, 87–95.

(7) Powell, C. E.; Qiao, G. G. Polymeric CO₂/N₂ Gas Separation Membranes for the Capture Carbon Dioxide from Power Plant Flue Gases. *J. Membr. Sci.* **2006**, *279*, 1–49.

(8) Choi, S.; Drese, J. H.; Jones, C. W. Adsorbent Materials for Carbon Dioxide Capture from Large Anthropogenic Point Sources. *ChemSusChem* **2009**, *2*, 796–854.

(9) Rubin, E. S.; Mantripragada, H.; Marks, A.; Versteeg, P.; Kitchin, J. The Outlook for Improved Carbon Capture Technology. *Prog. Energy Combust. Sci.* **2012**, *38*, 630–671.

(10) Song, C. Global Challenges and Strategies for Control, Conversion, and Utilization of CO₂ for Sustainable Development Involving Energy, Catalysis, Adsorption, and Chemical Processing. *Catal. Today* **2006**, *115*, 2–32.

(11) Gray, M. L.; Soong, Y.; Champagne, K. J.; Baltrus, J.; Stevens, R. W.; Toochinda, P. S., Jr.; Chuang, S. C. CO₂ Capture by Amine-Enriched Fly Ash Carbon Sorbents. *Sep. Purif. Technol.* **2004**, *35*, 31–36.

(12) Bollini, P.; Didas, S. A.; Jones, C. W. Amine–Oxide Hybrid Materials for Acid Gas Separations. *J. Mater. Chem.* **2011**, *21*, 15100–15120.

(13) Burkett, S. L.; Sims, D. D.; Mann, S. Synthesis of Hybrid Inorganic–Organic Mesoporous Silica by Co-Condensation of Siloxane and Organosiloxane Precursors. *Chem. Commun.* **1996**, *11*, 1367–1368.

(14) Beck, J. S.; Vartuli, J. C.; Roth, W. J.; Leonowicz, M. E.; Kresge, C. T.; Schmitt, K. D.; Chu, C. T. W.; Olson, D. H.; Sheppard, E. W.; McCullen, S. B.; Higgins, J. O.; Schlenker, J. L. A New Family of Mesoporous Molecular Sieves Prepared with Liquid Crystal Templates. *J. Am. Chem. Soc.* **1992**, *114*, 10834–10843.

(15) Franchi, R. S.; Harlick, P. J. E.; Sayari, A. Applications of Pore-Expanded Mesoporous Silica. 2. Development of a High-Capacity, Water-Tolerant Adsorbent for CO₂. *Ind. Eng. Chem. Res.* **2005**, *44*, 8007–8013.

(16) Xu, X. C.; Song, C. S.; Andresen, J. M.; Miller, B. G.; Scaroni, A. W. Novel Polyethyleneimine Modified Mesoporous Molecular Sieve of MCM-41 Type as Adsorbent for CO₂ Capture. *Energy Fuels* **2002**, *16*, 1463–1469.

(17) Hicks, J. C.; Drese, J. H.; Fauth, D. J.; Gray, M. L.; Qi, G.; Jones, C. W. Designing Adsorbents for CO₂ Capture from Flue Gas-Hyperbranched Aminosilicas Capable of Capturing CO₂ Reversibly. *J. Am. Chem. Soc.* **2008**, *130*, 2902–2903.

(18) Drese, J. H.; Choi, S.; Didas, S. A.; Bollini, P.; Gray, M. L.; Jones, C. W. Effect of Support Structure on CO₂ Adsorption Properties of Pore-Expanded Hyperbranched Aminosilicas. *Microporous Mesoporous Mater.* **2012**, *151*, 231–240.

(19) Drese, J. H.; Choi, S.; Lively, R. P.; Koros, W. J.; Fauth, D. J.; Gray, M. M. L.; Jones, C. W. Synthesis–Structure–Property Relationships for Hyperbranched Aminosilica CO₂ Adsorbents. *Adv. Funct. Mater.* **2009**, *19*, 3821–3832.

(20) Evans, J.; Zaki, A. B.; El-Sheikh, M. Y.; El-Safty, S. A. Incorporation of Transition-Metal Complexes in Functionalized Mesoporous Silica and Their Activity Toward the Oxidation of Aromatic Amines. *J. Phys. Chem. B* **2000**, *104*, 10271–10281.

- (21) Kramer, J.; Garcia, A. R.; Driessen, W. L.; Reedijk, J. Tuning the Recovery of an Rh-containing Catalyst with Silica-based (poly) Amine Ion Exchangers. *Chem. Commun.* **2001**, 23, 2420–2421.
- (22) Walcarius, A.; Etienne, M.; Bessiere, J. Rate of Access to the Binding Sites in Organically Modified Silicates. 1. Amorphous Silica Gels Grafted with Amine or Thiol Groups. *Chem. Mater.* **2002**, 14, 2757–2766.
- (23) Voss, R.; Thomas, A.; Antonietti, M.; Ozin, G. A. Synthesis and Characterization of Highly Amine Functionalized Mesoporous Organosilicas by an “All-in-One” Approach. *J. Mater. Chem.* **2005**, 15, 4010–4014.
- (24) D’Alessandro, D. M.; Smit, B.; Long, J. R. Review: Carbon Dioxide Capture: Prospects for New Materials. *Angew. Chem., Int. Ed.* **2010**, 49, 6058–6082.
- (25) Jones, C. W. CO₂ Capture from Dilute Gases as a Component of Modern Global Carbon Management. *Annu. Rev. Chem. Biomol. Eng.* **2011**, 2, 31–52.
- (26) Tsuda, T.; Fujiwara, T.; Taketani, Y.; Saegusa, T. Amino Silica Gels Acting as a Carbon Dioxide Absorbent. *Chem. Lett.* **1992**, 21, 2161–2164.
- (27) Hedin, N.; Chen, L.; Laaksonen, A. Sorbents for CO₂ Capture from Flue Gas—Aspects from Materials and Theoretical Chemistry. *Nanoscale* **2010**, 2, 1819–1841.
- (28) Long, W.; Brunelli, N. A.; Didas, S. A.; Ping, E. W.; Jones, C. W. Aminopolymer-Silica Composite-Supported Pd Catalysts for Selective Hydrogenation of Alkynes. *ACS Catal.* **2013**, 3, 1700–1708.
- (29) Kandel, K.; Althaus, S. M.; Althaus, P.; Peeraphatdit, C.; Kobayashi, T.; Trewyn, B. G.; Pruski, M.; Slowing, I. I. Solvent-Induced Reversal of Activities between Two Closely Related Heterogeneous Catalysts in the Aldol Reaction. *ACS Catal.* **2013**, 3, 265–271.
- (30) Brunelli, N. A.; Jones, C. W. Tuning Acid–Base Cooperativity to Create Next Generation Silica-supported Organocatalysts. *J. Catal.* **2013**, 308, 60–72.
- (31) Bollini, P.; Brunelli, N. A.; Didas, S. A.; Jones, C. W. Dynamics of CO₂ Adsorption on Amine Adsorbents. 1. Impact of Heat Effects. *Ind. Eng. Chem. Res.* **2012**, 51, 15145–15152.
- (32) Bollini, P.; Brunelli, N. A.; Didas, S. A.; Jones, C. W. Dynamics of CO₂ Adsorption on Amine Adsorbents. 2. Insights into Adsorbent Design. *Ind. Eng. Chem. Res.* **2012**, 51, 15153–15162.
- (33) Veneman, R.; Li, Z. S.; Hogendoorn, J. A.; Kersten, S. R. A.; Brilman, D. W. F. Continuous CO₂ Capture in a Circulating Fluidized Bed Using Supported Amine Sorbents, Brilman. *Chem. Eng. J.* **2012**, 207–208, 18–26.
- (34) Lively, R. P.; Chance, R. R.; Kelley, B. T.; Deckman, H. W.; Drese, J. H.; Jones, C. W.; Koros, W. J. Hollow Fiber Adsorbents for CO₂ Removal from Flue Gas. *Ind. Eng. Chem. Res.* **2009**, 48, 7314–7324.
- (35) Labreche, Y.; Lively, R. P.; Rezaei, F.; Chen, G.; Jones, C. W.; Koros, W. J. Post-Spinning Infusion of Poly(ethyleneimine) into Polymer/Silica Hollow Fiber Sorbents for Carbon Dioxide Capture. *Chem. Eng. J.* **2013**, 221, 166–175.
- (36) Rezaei, F.; Lively, R. P.; Labreche, Y.; Chen, G.; Fan, Y.; Koros, W. J.; Jones, C. W. Aminosilane-Grafted Polymer/Silica Hollow Fiber Adsorbents for CO₂ Capture from Flue Gas. *ACS Appl. Mater. Interfaces* **2013**, 5, 3921–3931.
- (37) Fan, Y.; Lively, R. P.; Labreche, Y.; Rezaei, F.; Koros, W. J.; Jones, C. W. Evaluation of CO₂ Adsorption Dynamics of Polymer/Silica Supported Poly(ethyleneimine) Hollow Fiber Sorbents in Rapid Temperature Swing Adsorption. *Int. J. Greenhouse Gas Control* **2014**, 21, 61–71.
- (38) Determan, M. D.; Hoysall, D. C.; Garimella, S. Heat- and Mass-Transfer Kinetics of Carbon Dioxide Capture Using Sorbent-Loaded Hollow Fibers. *Ind. Eng. Chem. Res.* **2011**, 51, 495–502.
- (39) Lively, R. P.; Mysona, J. A.; Chance, R. R.; Koros, W. J. Formation of Defect-Free Latex Films on Porous Fiber supports. *ACS Appl. Mater. Interfaces* **2011**, 3, 68–82.
- (40) Lee, J. S.; Hildesheim, P. C.; Huang, D.; Lively, R. P.; Oh, K. H.; Dai, S.; Koros, W. J. Hollow Fiber-Supported Designer Ionic Liquid Sponges for Post-Combustion CO₂ Scrubbing. *Polymer* **2012**, 53, 5906–5816.
- (41) Kovacic, P. Bisalkylation Theory of Neoprene Vulcanization. *Ind. Eng. Chem.* **1955**, 47, 1090–1094.
- (42) Wang, Y.; Jiang, L.; Matsuura, T.; Chung, T. S.; Goh, S. H. Investigation of the Fundamental Differences between Polyamide-Imide (PAI) and Polyetherimide (PEI) Membranes for Isopropanol Dehydration via Pervaporation. *J. Membr. Sci.* **2008**, 318, 217–226.
- (43) Robertson, G. P.; Guiver, M. D.; Yoshikawa, M.; Brownstein, S. Structural Determination of Torlon 4000T Polyamide-Imide by NMR Spectroscopy. *Polymer* **2004**, 45, 1111–1117.
- (44) Fritsch, D.; Peinemann, K. V. Novel Highly Permselective 6F-poly(amide-imide)s as Membrane Host for Nano-Sized Catalysts. *J. Membr. Sci.* **1995**, 99, 29–38.
- (45) Chafin, R. W. II. Torlon and Silicalite Mixed Matrix Membrane for Xyleneisomer Purification. Ph.D. Dissertation, Georgia Institute of Technology, Atlanta, GA, 2007.
- (46) Kosuri, M. R. Polymeric Membranes for Super Critical Carbon Dioxide (scCO₂) Separations. Ph.D. Dissertation, Georgia Institute of Technology, Atlanta, GA, 2009.
- (47) Kosuri, M. R.; Koros, W. J. Defect-Free Asymmetric Hollow Fiber Membranes from Torlon, a Polyamide-Imide Polymer, for High-Pressure CO₂ Separations. *J. Membr. Sci.* **2008**, 320, 65–72.
- (48) Ultem Resin 1010 data sheet, Sabic Innovative Plastics.
- (49) Wang, Y.; Goh, S. H.; Chung, T. S. Miscibility Study of Torlon Polyamide-Imide with Matrimid 5218 Polyimide and Polybenzimidazole. *Polymer* **2007**, 48, 2901–2909.
- (50) Chung, T. S.; Chan, S. S.; Wang, R.; Lu, Z. H.; He, C. H. Characterization of Permeability and Sorption in Matrimid/C60 Mixed Matrix Membranes. *J. Membr. Sci.* **2003**, 211, 91–99.
- (51) Qiao, X.; Chung, T. S. Diamine Modification of P84 Polyimide Membranes for Pervaporation Dehydration of Isopropanol. *AIChE J.* **2006**, 52, 3462–3472.
- (52) Yuan, J.; Dunn, D.; Clipse, N. M.; Newton, R. J. Formulation Effects on the Thermomechanical Properties and Permeability of Free Films and Coating Films: Characterization of Cellulose Acetate Films. *Pharm. Technol.* **2009**, 33, 88–100.
- (53) Xu, X. C.; Song, C. S.; Andresen, J. M.; Miller, B. G.; Scaroni, A. W. Preparation and Characterization of Novel CO₂ “Molecular Basket” Adsorbents Based on Polymer-Modified Mesoporous Molecular Sieve MCM-41. *Microporous Mesoporous Mater.* **2003**, 62, 29–45.
- (54) Satyapal, S.; Filburn, T.; Trela, J.; Strange, J. Performance and Properties of a Solid Amine Sorbent for Carbon Dioxide Removal in Space Life Support Applications. *Energy Fuels* **2001**, 15, 250–255.
- (55) Delaney, S. W.; Knowles, G. P.; Chaffee, A. L. Hybrid Mesoporous Materials for Carbon Dioxide Separation. *Am. Chem. Soc., Div. Fuel Chem., Prepr. Pap.* **2002**, 47, 65–66.
- (56) Yue, M. B.; Sun, L. B.; Cao, Y.; Wang, Z. J.; Wang, Y.; Yu, Q.; Zhu, J. H. Promoting the CO₂ Adsorption in the Amine-Containing SBA-15 by Hydroxyl Group. *Microporous Mesoporous Mater.* **2008**, 114, 74–81.
- (57) Heldebrandt, D. J.; Jessop, P. G. Liquid Poly(ethylene glycol) and Supercritical Carbon Dioxide: A Benign Biphasic Solvent System for Use and Recycling of Homogeneous Catalysts. *J. Am. Chem. Soc.* **2003**, 125, 5600–5601.
- (58) Zhang, J.; Han, B.; Zhao, Y.; Li, J.; Hou, M.; Yang, G. CO₂ Capture by Hydrocarbon Surfactant Liquids. *Chem. Commun.* **2011**, 47, 1033–1035.
- (59) Pesek, S. C.; Koros, W. J. Aqueous Quenched Asymmetric Polysulfone Hollow Fibers Prepared by Dry/Wet Phase Separation. *J. Membr. Sci.* **1994**, 88, 1–19.
- (60) Li, G.; Xiao, P.; Xu, D.; Webley, P. A. Dual Mode Roll-up Effect in Multicomponent Non-Isothermal Adsorption Processes with Multilayered Bed Packing. *Chem. Eng. Sci.* **2011**, 66, 1825–1834.
- (61) Lively, R. P.; Chance, R. R.; Mysona, J. A.; Babu, V. P.; Deckman, H. W.; Leta, D. P.; Thomann, H.; Koros, W. K. CO₂ Sorption and Desorption Performance of Thermally Cycled Hollow Fiber Sorbents. *Int. J. Greenhouse Gas Control* **2012**, 10, 285–294.

(62) Yue, M. B.; Chun, Y.; Cao, Y.; Dong, X.; Zhu, J. H. CO₂ Capture by As-Prepared SBA-15 with an Occluded Organic Template. *Adv. Funct. Mater.* **2006**, *16*, 1717–1722.

(63) Amundsen, T. G.; Oi, L. E.; Eimer, D. A. Density and Viscosity of Monoethanolamine + Water + Carbon Dioxide from (25 to 80) °C. *J. Chem. Eng. Data* **2009**, *54*, 3096–3100.

(64) Drage, T. C.; Arenillas, A.; Smith, K. M.; Snape, C. E. Thermal Stability of Polyethylenimine Based Carbon Dioxide Adsorbents and Its Influence on Selection of Regeneration Strategies. *Microporous Mesoporous Mater.* **2008**, *116*, 504–512.

(65) Sayari, A.; Belmabkhout, Y.; Da'na, E. CO₂ Deactivation of Supported Amines: Does the Nature of Amine Matter? *Langmuir* **2012**, *28*, 4241–4247.

(66) Zhang, Z. H.; Ma, X. L.; Wang, D. X.; Song, C. S.; Wang, Y. G. Development of Silica-Gel-Supported Polyethylenimine Sorbents for CO₂ Capture from Flue Gas. *AIChE J.* **2012**, *58*, 2495–2502.

(67) Xu, X.; Song, C.; Miller, B. G.; Scaroni, A. W. Influence of Moisture on CO₂ Separation from Gas Mixture by a Nanoporous Adsorbent Based on Polyethylenimine-Modified Molecular Sieve MCM-4. *Ind. Eng. Chem. Res.* **2005**, *44*, 8113–8119.

(68) van den Berg, G. B.; Smolders, C. A. Diffusional Phenomena in Membrane Separation Processes. *J. Membr. Sci.* **1992**, *73*, 103–118.